Proceedings of FBC2005
18th International Conference on Fluidized Bed Combustion
May 22-25, 2005, Toronto, Ontario, Canada

FBC2005-78092

AN INVESTIGATION ON LOW-TEMPERATURE FLUIDIZED COMBUSTION OF LIQUID FUELS

Lorenzo Ferrante
Dip. Ingegneria Chimica ed Alimentare
Università di Salerno
Via Ponte Don Melillo
Fisciano (SA), 84084, Italy
e-mail: lferrante@unisa.it

Michele Miccio
Dip. Ingegneria Chimica ed Alimentare
Università di Salerno
Via Ponte Don Melillo
Fisciano (SA), 84084, Italy
e-mail: mmiccio@unisa.it

Roberto Solimene
Dip. Ingegneria Chimica
Università degli Studi di Napoli
P.le Tecchio N.80
Napoli, 80125, Italy
e-mail: rsolimen@unina.it

Francesco Miccio
Istituto Ricerche sulla Combustione
Consiglio Nazionale delle Ricerche
Via Metastasio N.17
Napoli (Na), 80125, Italy
e-mail: miccio@irc.na.cnr.it

ABSTRACT

Presently, the combustion at low temperature is receiving a great deal of interest because emissions of micro- and nano-pollutants are expected to be greatly reduced.

Following previous studies on the low temperature combustion behavior, the authors report results and discussion of steady-state experiments on an atmospheric, pre-pilot scale, 140 mm ID, FB reactor, equipped with an under-bed, air-assisted, liquid-fuel injector. The experimental program was focused on the operation at temperatures lower than the classical value for FBC of solid fuels (i.e., 850°C). The data series taken into consideration are the concentrations of the main unburned species in the splash zone, those of oxygen measured in the bed and in the splash zone as well as the freeboard pressure.

The interpretation of the results is mainly based on the statistical analysis in the time domain. The combustion pattern of bio-diesel is compared to that of the diesel fuel under varying operating conditions (e.g., bed temperature, dispersion air velocity at the fuel nozzle, injector height in the bed). Conclusions that were previously published on the base of lab-scale results are checked against new data obtained on the pilot scale. An innovative technique for the analysis of the micro–explosive regime is presented. It consists in the comparison of oxygen concentration measured by the zirconia-based probes at different heights in the bed and in the splash region, pressure signals measured in the freeboard and purposely filtered, and video-recordings of the bed surface phenomena.

INTRODUCTION

From a viewpoint directed at application of fluidized bed combustion (FBC), conventional, petroleum-derived liquid fuels are usually not taken into consideration. Vice versa, the cheap biomass-derived liquid fuels are worth of being exploited, at least for some specific applications.

The combustion at low temperature is presently receiving a great deal of interest in view of depressing emission of micro- and nano-pollutants. The operation of a fluidized bed combustor (FBC) at a temperature lower than the classical value for FBC of solid fuels (i.e., 850°C) presents a number of interesting issues the mechanisms of which are not completely revealed yet. The combustion of a liquid fuel in a fluidized bed can be considered as the result of a number of serial stages: atomization, vaporization, pyrolysis, mixing with air and oxidation, formation of pollutant. They occur in an ideal sequence moving from the fuel inlet port to the bed exit, provided that the residence time in the bed is long enough [1]. Otherwise, diffusion flames take place above the bed as soon as fuel-rich sockets are released and ignited [2]. These flames have a transient behavior, a short life and at T<850°C give rise to localized micro-explosions. The combustion pattern of a liquid fuel (i.e., gas oil) in the 550-700°C temperature range was investigated by Miccio et al. [2] at the laboratory scale, i.e., with an 80 mm ID fluidized combustor. They identified a combustion behavior at a bed temperature below 750°C that was described as “regime with micro-explosions”. Because of the periodic eruption of air bubbles the properties of the

system are dramatically time-dependent and the combustion scenario is complex.

Passive measurements of pressure signals represent another tool contributing to the knowledge of the phenomena occurring inside the reactor. The application of pressure or acoustic probes to fluidized beds is a well-established technique for studying and characterizing the bed fluid dynamics under non-reactive conditions [3]. Acoustic signals generated during premixed FB combustion of gaseous hydrocarbons were taken into consideration and comprehensively investigated by Zukowsky [4-6]. Transient pressure profiles were recorded, showing a huge distribution of pressure peaks that were attributed to explosions. That analysis demonstrated that the combustor exhibited an explosive behavior in a large temperature range,

More recently, Bulewicz et al. [7] introduced a technique based on video recordings of the bed surface and on image analysis in three color bands to investigate the explosive behavior in the lab-scale, premixed combustion of methane.

In the above cases, also zirconia-based solid-state sensors turn out useful. They have been used in fluidized beds by a large number of investigators [8-11] whenever information concerning spatial or dynamic changes of the oxygen concentration is relevant for the understanding of the process phenomena. By means of zirconia-based sensors with fast time response, Solimene et al. [12] have been able to study gas mixing phenomena inside the bed as well in the splash zone with high accuracy and temporal resolution.

The present paper extends the previous investigation [2] to the pilot scale, where some drawbacks (e.g., slugging) or limitations (e.g., size of the fuel injection nozzle) posed by the lab scale could be overcome. To this end an atmospheric 140 mm ID fluidized combustor has been used. The previously found influence of the bed temperature was subjected to a confirmation. New conditions concerning fuel injection were explored. Finally, the chemical nature of the fuel was varied. Results in terms of both data series and time-averaged concentrations of the main reaction intermediate (CH_4) and the main unburned species (CO) are discussed. Based on the comparison of measurements of oxygen concentration by zirconia-based probes in the bed and in the splash region, pressure signals in the freeboard and video-recordings of the bed surface, a new technique for the analysis of the micro–explosive regime is also presented.

NOMENCLATURE

D_{be}	endogenous bubble diameter	m
D	molecular diffusion coefficient	m^2/s
d_0	nozzle diameter	m
d_p	particle diameter	m
d_t	bed diameter	m
F	Faraday constant	
g	gravitational acceleration	m/s^2
H_{eb}	expanded bed height	m
H_{mf}	bed height at minimum fluidization	m
K_{BC}	coefficient of gas interchange between bubble and cloud-wake region	s^{-1}
K_{CE}	coefficient of gas interchange between emulsion phase and cloud-wake region	s^{-1}
K_{BE}	coefficient of gas interchange between bubble and emulsion phase	s^{-1}
n	electrons involved in the electrochemical reaction	
P	pressure	Pa
Q_0	vol. flow rate of atomization air	m^3/s
R	ideal gas constant – 8314 J/(kmol*K)	
T	bed temperature	K
T_{ZrO2}	ZrO2 sensor tip temperature	K
u_0	air velocity at the fuel nozzle	m/s
U	fluidization velocity	m/s
U_{be}	endogenous bubble velocity	m/s
U_{mf}	minimum fluidization velocity	m/s
U_{ZrO2}	electromotive force	mV
U^0_{ZrO2}	the electromotive force corresponding to $y_{O_2} = y^{rif}_{O_2}$	mV
V_{b0}	fuel bubble volume at the nozzle	m^3
X_b	crossflow ratio	-
y_{O_2}	oxygen molar fraction in the investigated gas	-
$y^{rif}_{O_2}$	oxygen molar fraction in the reference gas	-
ε	voidage into the bed	-
$ε_{mf}$	voidage at minimum fluidization	-

EXPERIMENTAL

Apparatus

An atmospheric bubbling fluidized-bed reactor (FBR140) has been used for experiments of steady-state combustion of liquid fuels (see Fig. 1). The fluidization column consists in two cylindrical stainless steel tubes, having 140 mm ID and 200 mm ID, respectively. A conical section in the middle of the fluidization column allows the gradual change of the size between the tubes. The first tube (1010 mm high) contains the bed and the splash zone, the second one (1800 mm high) is the disengaging region. The reactor can work at operating temperatures up to 900°C thanks to electrical heating that is supplied by radiant shells installed along the fluidization column for a total height of 2 m. The fluidizing gas can be pre-heated up to 500°C and then fed to an air plenum. The air distributor consists in a reversed cone filled with 3/8" AISI 304 spheres to even the flow out.

The liquid fuel is metered by means of a membrane pump (KNF Stepdos type). The mass flow rate is measured by the mass variation of the fuel vessel mounted on a digital balance. A horizontal, water-cooled fuel injector is located at a height of 140 mm above the flange between the reversed cone and the fluidization column. The liquid fuel is injected into the bed through a two-fluid, 2 mm ID nozzle with the aid of a dispersion air stream. The flow rates of the fluidizing gas and the dispersion air are measured by rotameters. Flue gases at the exit of the fluidization column move to a cyclone and then to the stack.

Gas sampling is accomplished by a cooled probe located at 480 mm above the air distributor or at the stack. The sampled gas goes in sequence through a filter, a heated tube, a

cooling unit, a pump and, finally, a battery of gas analyzers for O_2, CO_2, CO, N_2O, NOx and CH_4. The pressure is measured in the freeboard by a transducer (Druck PTX type, 0-100 mbar range, 1 kHz sampling rate) characterized by a fast time response and connected to the freeboard by means of a wave-guide made by a 6 mm ID stainless steel tube. This set-up allows measurement of dynamic pressure at a height of 1 m above the air distributor.

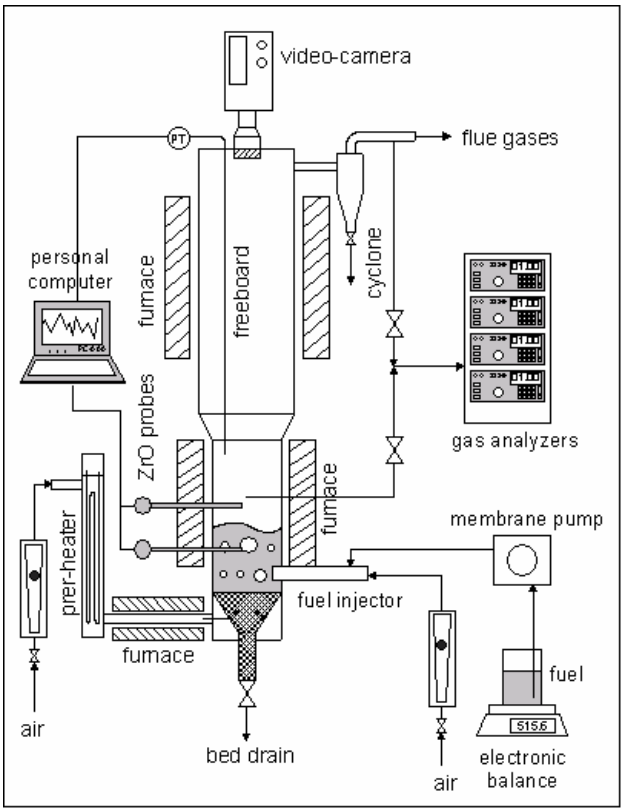

Figure 1: Schematic of the FBR140 experimental facility.

A video camera (Philips AG-DVX102A, 25 fps frame rate) connected to a video-recorder is mounted on the top of the fluidization column and allows the bed surface to be observed via an optical window.

The fluidization column is also equipped with three zirconia-based probes (SIRO2 C700 + DS probe) to measure oxygen concentration along the reactor. The adopted oxygen solid state sensor is custom-made and it is characterized by a zirconia-based cylindrical pellet, 4 mm dia. and 3 mm long, sealed at the end of a 6 mm dia. alumina tube. The small size of the sensor tip determines a response time lower than 10 ms following a change in oxygen concentration. An R-type thermocouple is kept in touch with the inner surface of the zirconia pellet to measure the sensor tip temperature. An electromotive force, U, is generated when the two sensor tip surfaces are exposed to gases at different oxygen concentration. The sensors are horizontally mounted in the bottom section of the fluidization column in order to position the sensor tips along the column axis at a height of 30, 330 and 480 mm above the distributor level, respectively. The simultaneous acquisition of sensor tip temperature and electromotive force allows estimating the oxygen concentration. The pressure and oxygen concentration signals are acquired by a data acquisition unit consisting in an A/D converter coupled with a PC and synchronized with the video recording system.

Technique

Silica sand (200-400 μm size range) is used as bed material the minimum fluidization velocity of which is about 0.049 m/s at a bed temperature of 650°C. The bed mass is 7 kg corresponding to a static bed height of 300 mm and to a bed aspect ratio, H_{mf}/d_t, of about 2.1. The liquid fuels investigated are a gas oil (diesel fuel) for automotive application, which was taken as the reference fuel, and a commercial bio-diesel as an alternative fuel.

When the fluidized bed reaches the temperature of about 500°C by external heating, fuel feeding into the reactor is started. The flow rates of the various streams, i.e., air and liquid fuel, are adjusted in order to achieve the desired steady-state condition. Temperatures, pressures, freeboard and flue gas concentrations are on-line monitored and recorded by the data acquisition system. Typically, once the steady-state condition of the pre-set combustion test is reached, all the measured variables are acquired for at least 30 min.

Two different hold-ups of spheres in the reverse cone used as air distributor are adopted in order to obtain two different heights of fuel injection with respect to the distributor level, i.e., 10 and 140 mm. These two positions will be referred to as “bottom injection” and “upper injection”, respectively, in the present paper.

Experiments are carried out at three different bed temperatures, i.e., 600, 650 and 700°C, and at a dispersion air velocity in the fuel injector nozzle, u_0, of about 100 m/s for both liquid fuels to compare the flue gas emissions of the two fuels. Another set of experiments using only gas oil as fuel is carried out at about 650°C and different values of u_0, i.e., 50, 100, 130 and 160 m/s, to investigate the effect of fuel injection condition on bed combustion efficiency. During these latter tests, the superficial fluidization velocity resulting from both the inlet air streams is maintained constant in spite of the changes in u_0. In all the tests, the overall air excess is set to achieve an oxygen concentration in the flue gas of about 5%.

RESULTS AND DISCUSSION

Data treatment

The time-resolved concentration measurements of the main reaction intermediate (CH_4) and the main unburned species (CO) as well as those of oxygen in the splash zone and in the flue gases, are shown in Fig. 2A, 2B and 2C, respectively, for a typical test burning gas oil. The observed signals highlight that methane, carbon monoxide and oxygen concentration exhibits fluctuations during a steady-state run of the FBR140 unit. These fluctuations cannot be simply attributed to statistic oscillations, measurement error and noise generated by signal handling/conversion. On the all, it can be speculated that the FB combustor (as a macroscopic system) is globally operated at a steady-state condition in the tested temperature range, whereas its reacting core, namely the bubbles and the splash zone, is in a dynamic condition. This

tends to confirm the pilot scale results previously obtained by Miccio et al. [2] on a bench-scale unit.

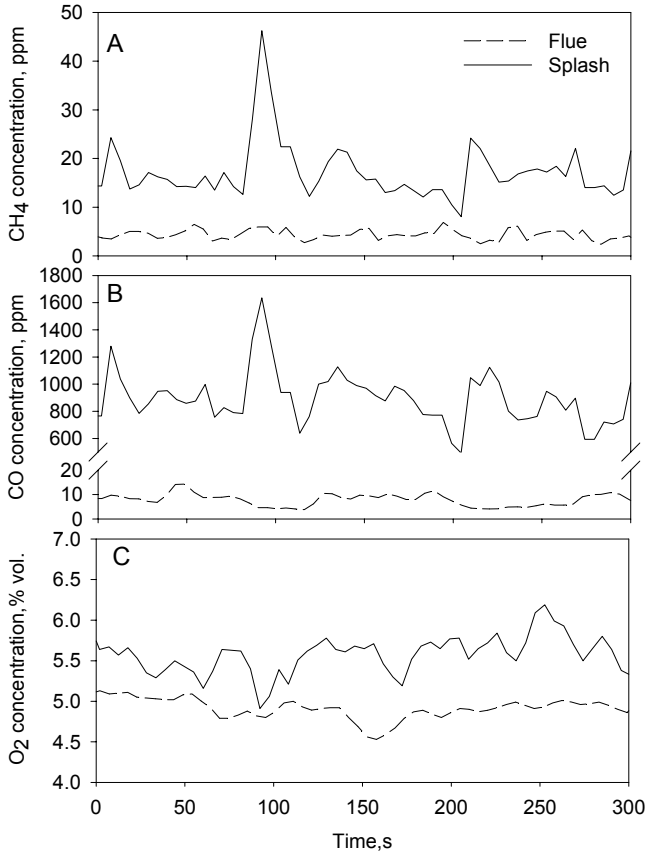

Figure 2. Time-resolved gas concentration measured in the splash zone and in the flue gas. A) methane concentration; B) carbon monoxide concentration; C) oxygen concentration
(fuel: gas oil, T=650°C, u_0=100m/s, bottom injection).

In order to ensure a better reliability, most of the results reported in the following discussion come from tests that were repeated at least twice. In any case, when gas concentrations at steady-state condition are taken into consideration, they are the time-averaged values of the measured fluctuating data series. On the other hand, the standard deviation of concentration signals was determined for each test and its value was considered as an index of the extent of fluctuations.

The acquired pressure signal has been elaborated by a high-pass filter (cut frequency: 80 Hz) in order to highlight pressure fluctuations associated with acoustic emissions due to micro-explosions [13] and to remove fluctuations associated with bubbling and characterized by low frequencies (1-10 Hz).

The signals of the oxygen solid-state sensors have been elaborated in the light of a Nernst-like equation that relates the electromotive force, U_{ZrO2}, to the oxygen concentration in the investigated gas [14]

$$U_{ZrO2} = U^0_{ZrO2} - \left(R * T_{ZrO2} \Big/ n * F \right) \ln \left(y_{O_2} \Big/ y^{rif}_{O_2} \right) \qquad \text{(eq.1)}$$

where R, T_{ZrO2}, F, n, y_{O_2}, $y^{rif}_{O_2}$ and U^0_{ZrO2} are the ideal gas constant, the sensor tip temperature, the Faraday constant, the electrons involved in the electrochemical reactions, the oxygen molar fraction in the investigated gas and in the reference gas and the electromotive force corresponding to $y_{O_2} = y^{rif}_{O_2}$, respectively.

Gas concentrations at bed exit

The analysis of the time-averaged values of gas composition in the splash zone and in the flue gas (Fig.2) highlights that:

i. the combustion process is not completed in the bed as it is made evident by the large concentrations of CH_4 and CO at the bed exit;
ii. post-combustion takes place in the freeboard as demonstrated by the concentration decrease of the unburned species.

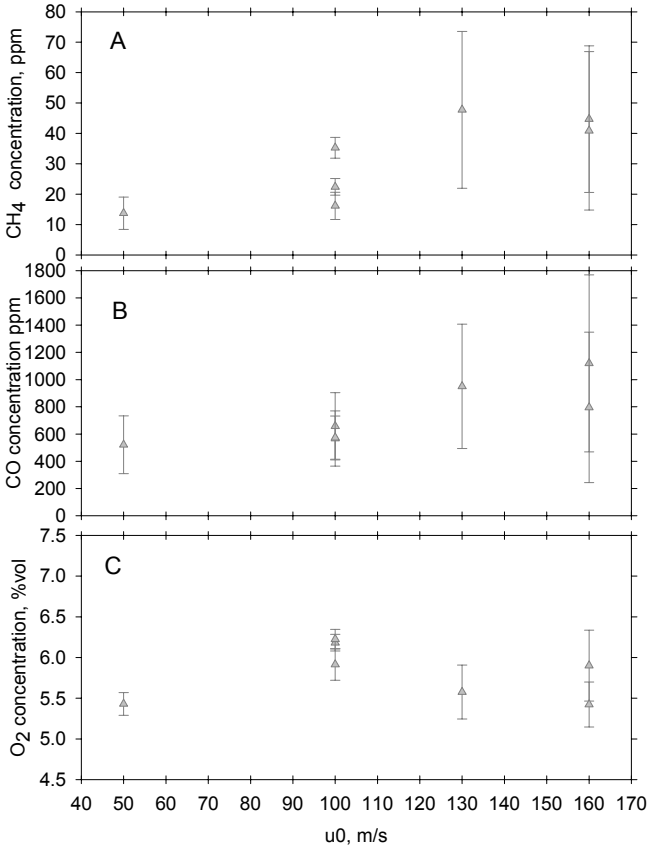

Figure 3 Averaged gas concentrations with standard deviation bars measured in the splash zone as a function of the dispersion air velocity at the fuel nozzle. A) methane concentration; B) carbon monoxide concentration; C) oxygen concentration
(fuel: gas oil, T=650°C, bottom injection).

Figure 3 reports the concentration of CH_4 (Fig. 3A), CO (Fig. 3B) and O_2 (Fig. 3C) measured in the splash zone as a function of the air velocity used for dispersion of the reference fuel, i.e., gas oil. The bed temperature (T=650°C), the injector position (i.e., "bottom injection"), the superficial fluidization velocity (U=0.312 m/s) and, as a consequence, the fuel feed rate have been maintained constant. For each experimental test a data point representing the average value of the measured concentration and the bar representing the double of the

standard deviation of the measured signal are reported in Fig. 3. The statistical treatment of the experimentally measured data series quite clearly demonstrates that the larger is the average value, the greater is the standard deviation of whatever gaseous concentration. This is a pretty reasonable finding in these types of measurement because of the occurrence of an intermittent and localized combustion pattern. Therefore, in order to investigate the overall trend and the macroscopic features of the liquid fuel burning, the actual fluctuations will not be considered anymore and the average values of the gaseous concentrations will be used in the present section.

The increase of the dispersion air velocity from u_0=50 to 160 m/s leads to a parallel growth of both CH_4 and CO concentrations under the "bottom" injector configuration, as can be seen from symbols (triangles) in Fig. 3A and B. In parallel, the O_2 concentration in Fig. 3C does not exhibit a so-evident trend owing to the difference in order of magnitude of the CH_4 and CO concentrations with respect to oxygen. The injection of air-atomized liquid fuels into the fluidized bed reactor generates "endogenous" bubbles [15-16], i.e., formed by rapid vaporization of the liquid fuel. Those bubbles are characterized by a high content of gaseous combustible species. A larger u_0 enhances the jet penetration [17], induces more intense fuel atomization and, likely, better fuel dispersion over the cross sectional area of the bed; in turn the air-fuel mixing and the fuel conversion are expected to augment. On the other hand, the initial size of the endogenous bubble [1] increases with u_0 up to the point a slugging regime [18] may establish above the injector position. So larger endogenous bubbles rise through the bed, their mass transfer rates with the dense phase are lower and the fuel–air mixing can become progressively poorer along the bed. In order to have a first assessment, the crossflow factor of the endogenous bubble, X_b, i.e., the product of the bubble residence time and the overall mass transfer coefficient between bubble and emulsion phase, K_{BE}, turns out useful [18]. The X_b values, which have been determined by the relationships reported in the Appendix, are reported in table 1. They clearly underline that the crossflow ratio and, hence, the extent of the fuel bubble–air mixing decrease as u_0 increases.

u_0, m/s	50	100	130	160
X_b	1.19	0.81	0.71	0.64

Table 1: Calculated values of the cross flow ratio for different dispersion air velocities.

Figure 4A reports the concentration of CH_4 measured in the splash zone as a function of bed temperature in the tested range (T=600-700°C), when maintaining constant the other operating conditions (i.e., gas oil as fuel; u_0; the excess fluidization velocity, $U-U_{mf}$). Firstly, it appears that CH_4 is considerably higher (e.g., about one order of magnitude) in the case of the "upper injection" than the "bottom" one. As the liquid fuel is vaporized very fast [1], the "upper injection" shortens the residence time that the fuel spends in the bed as gaseous phase: as a consequence, conversion of the fuel is reduced in the bed and delayed to the splash zone. Secondly, a larger spread in CH_4 concentration is evident in the case of "upper injection" (see the symbols of the duplicate tests). Again, such a spread is to be related to fuel post-combustion in the splash zone. In particular, it is likely that endogenous bubbles leave the bed with a larger CH_4 content, inducing greater fluctuations of CH_4 concentration in the splash zone. As a consequence, the gas sampling carried out by a fixed-position probe is characterized by a worse reproducibility in the duplicate tests.

Figure 4B reports the CO concentration as a function of bed temperature for the same tests considered in Fig. 4A. Clearly, the comparison between the measurements of CO obtained by the "bottom" and the "upper injection" confirms the previously discussed behavior of CH_4. Altogether, the pattern exhibited in parallel by CO and CH_4 is in agreement with the previous finding [2] that either one of the gas species is fully representative of the burning loss and can be selected as an indicator for the investigation of the combustion mechanism. Finally, Figure 4C reports the O_2 concentration as a function of bed temperature for the same tests as above and shows a very similar trend.

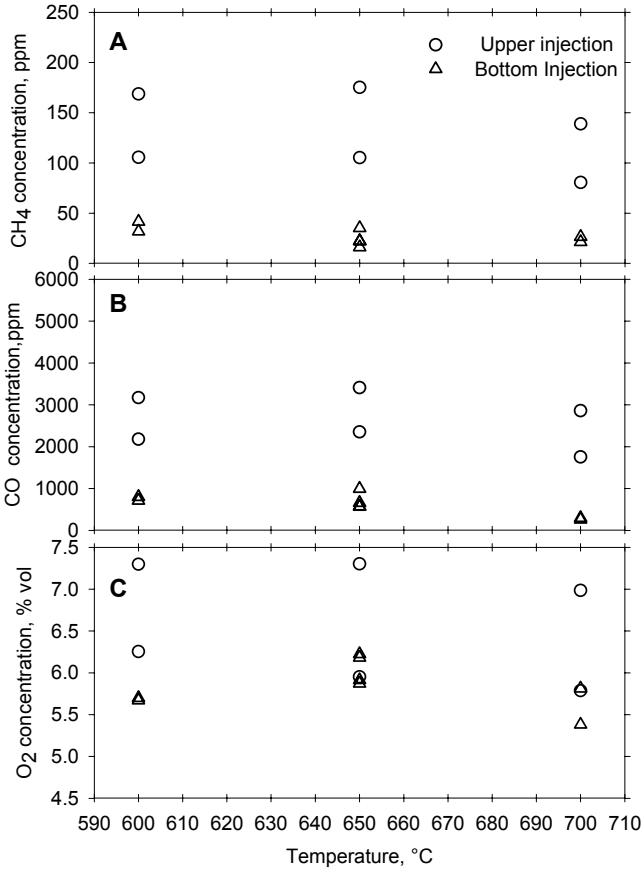

Figure 4 Averaged gas concentration measured in the splash zone for different bed temperatures and injection position. A) Methane concentration; B) carbon monoxide concentration; C) oxygen concentration
(fuel: gas oil, T=650°C, u_0=100 m/s).

In the "upper injection" case carbon monoxide and methane exhibit a pattern that seems to show a maximum value at T=650°C in the tested temperature range. Instead, oxygen concentration slightly decreases as the bed temperature increases. On the other hand, in the "bottom

injection" case the concentration of the CO and CH_4 shows a slight decreasing pattern, whereas oxygen concentration again exhibits a non monotonic trend. Altogether, these results represent a partial confirmation of the findings obtained by Miccio et al. [2] in their lab-scale experiments.

Figure 5 reports the concentration of CH_4 (Fig. 5A), CO (Fig. 5B) and O_2 (Fig. 5C) measured in the splash zone as a function of bed temperature during experiments carried out with bio-diesel. The bed temperature range (600-700°C), the fuel injection conditions as well as the other operating settings were exactly the same of those used in the tests carried out with gas oil. The bio-diesel presents just the same behavior of the gas oil; in particular, the CO and CH_4 concentrations are higher in the case of "upper injection" and exhibit a non-monotone trend as a function of the bed temperature, whereas a decreasing pattern is evident during the "bottom injection" mode.

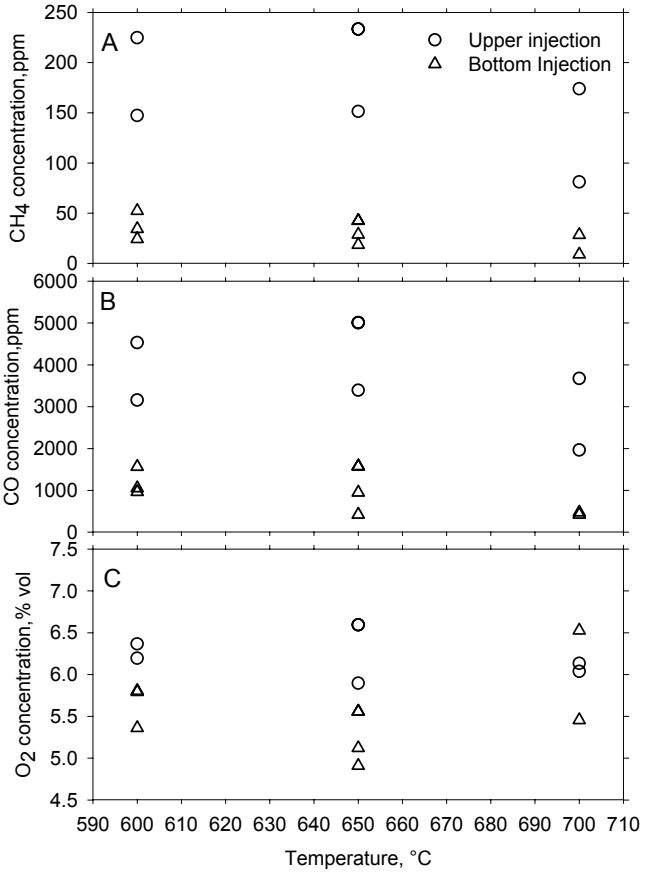

Figure 5 Averaged gas concentration measured in the splash zone for different bed temperatures and injection position. A) methane concentration; B) carbon monoxide concentration; C) oxygen concentration
(fuel: bio-diesel, T=650°C, u_0=100 m/s).

By comparing the results presented in both Figs. 4 and 5 for gas oil and bio-diesel, it turns out that the bio-diesel always exhibits higher levels of unburned species concentration. At the present state of the investigation, it can be only argued that differences due to the physical-chemical nature of the fuel may have a relevant role. For instance, the atomization behavior downstream from the injection nozzle or the kinetic mechanism of oxidation might be dissimilar for the two fuels, leading to larger emissions of carbon monoxide and methane from the top of the bed for the bio-diesel.

For both bio-diesel and gas oil, the above discussion suggests the conclusion that in the tested range of bed temperature (600-700°C) the post-combustion reactions are truly relevant in the splash zone. This latter, therefore, must be regarded as a further reactor for fuel oxidation past the bed zone and it must be taken in the due consideration in every effort leading to the understanding of the combustion mechanism or simulation of the low-temperature combustion process.

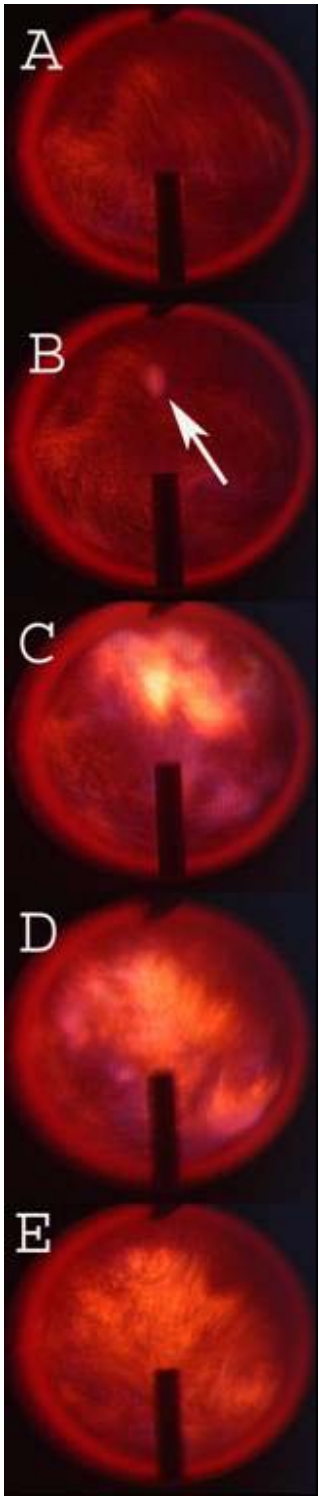

Figure 6: Sequence of frames representing the bed surface recorded from the top of the fluidization column during the occurrence of a micro-explosion
(fuel: bio-diesel, T=650°C, u_0=100 m/s, bottom injection, frame rate: 25 fps).

Phenomenology

The combustion phenomenology has been investigated by the visual observation of the bed surface carried out by means of a video camera located at the top of the fluidization column. Figure 6 reports a typical sequence of frames acquired during the occurrence of a micro-explosion under typical operating conditions. (T=650°C, fuel: bio-diesel, u_0=100 m/s, bottom injection, frame rate: 25 fps). The bed and the fluidization column are hot enough so that the emitted red radiation ensures a satisfactory luminosity. Figure 6A shows the bed surface under bubbling conditions: the darker areas correspond to the emulsion phase, whereas the lighter ones to the bubbles during the eruption. The next four slides (Fig. 6B-E) show the rapid generation and extinction of a light flash (white-colored area),

which is indicated by the arrow in Fig. 6B. The flash is determined by a micro-explosion that also generates acoustic effects. In the figures 6C and D it is also evident that blue-colored flames begin to appear just after the light flash. The observed frame sequence suggests that a single micro-explosion does not cover the entire bed section and seems to begin below the bed surface. Events of this kind appear very frequently in the video recording and can be considered typical of the combustor behavior under the operating conditions reported here.

In conclusion, the visual observation of the bed surface and the analysis of the video recording provide a further confirmation of the combustion "regime with micro-explosions" previously reported by the authors [2] on the bench scale. The results are also in agreement with the phenomenology described in details by Bulewicz and coworkers [7], with reference to the premixed combustion of methane in a lab-scale, bubbling fluidized bed of sand.

Time-resolved and synchronized measurements

Figure 7 reports typical time series of oxygen concentration (Fig. 7A, B and D) measured by the zirconia-based probes at the height of 30 and 330 mm in the bed, and 480 mm in the splash region, respectively, as well as the filtered pressure signal measured in the freeboard. The signals were synchronized with a video recording taken in the same 6 s time window during a steady-state combustion test of bio-diesel at T = 650°C, u0 = 100 m/s, "bottom injection" mode.

The oxygen concentration profile measured in the splash zone (Fig. 7A), i.e., at about 80 mm above the bed surface, clearly highlights the characteristic fluctuations generated by the combustion of a liquid fuel in a fluidized bed at low temperature. The average value of the molar fraction in the observed time window is about 5.6%, but sometimes the concentration abruptly decreases underlining the presence of oxygen-starving zones. The time-resolved oxygen concentration measured inside the bed (Fig. 7B), i.e., 70 mm below the bed surface, shows a qualitatively similar trend. However, the time-averaged value is 5.8%, i.e., slightly higher; the fluctuations are wider; and the time intervals characterized by oxygen concentration approaching to zero are more frequent and longer. Besides, the signal in Fig. 7A seems to be well cross-correlated to that one in Fig. 7B, showing a time lag of about 0.25 s.

The high-pass filtered component of the pressure time series measured in the freeboard (Fig. 7C) highlights the occurrence of micro-explosion events with their intensity and frequency. The vertical lines plotted in Figs. 7B and 7C mark the time instants corresponding to the detection of a micro-explosion by the start-up of a new, quickly smoothed pressure wave. The frequency of micro-explosions has been evaluated to be about 3-4 Hz.

However, the pressure measurement technique does not allow the spatial location of the micro-explosions to be exactly recognized. In order to do so, the comparison of the high-pass filtered pressure signal with the video recording and oxygen fluctuations can be useful. The continuous vertical lines plotted in the Figs 7B and C correspond to those micro-explosions that just match the light flashes detected by the frame-by-frame inspection of the related video recording. It is evident that: i) most of the micro-explosions are detected by either technique; ii) a few (and generally less intense) ones are only recognized by the pressure-based technique (dashed vertical lines). In this latter case the micro-explosive phenomenon probably takes place inside the bed. On the other hand, the analysis of oxygen molar fraction measured just below the bed surface shows that each sudden drop of the O_2 concentration in Fig. 7B well corresponds to the onset of a new pressure wave in Fig. 7C, even in the cases a light flash is not observed.

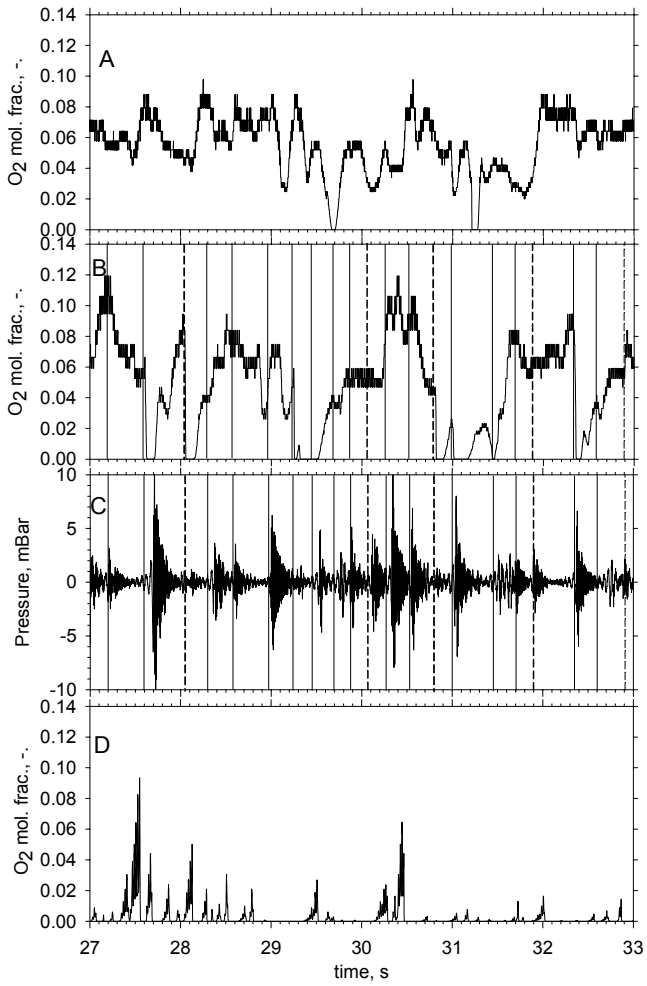

Figure 7: Time-resolved pressure and oxygen concentration signals during a bio-diesel combustion test. A) oxygen concentration measured at 480 mm above the air distributor; B) oxygen concentration measured at 330 mm above the air distributor; C) high-pass filtered pressure measured in the freeboard; D) oxygen concentration measured at 30 mm above the air distributor;
(fuel: bio-diesel, T=650°C, u_0=100 m/s, bottom injection)

The time-resolved oxygen concentration at the fuel injection level is reported in Fig. 7D. The oxygen molar fraction is about zero for most of the time. This finding is difficult to be interpreted; it can only be speculated that the probe tip sampled gases from the jet-generated flare, i.e., an oxygen-starving zone, for most of the time.

CONCLUSIONS

i. An increase of the dispersion air velocity u_0 leads to a parallel growth of the main reaction intermediate (CH_4) and the main unburned species (CO) concentrations in the splash region under the "bottom" injector configuration. This has been related to a poorer fuel–air mixing inside the bed, as quantitatively documented by the determination of the crossflow ratio.

ii. The bio-diesel presents just the same behavior of the gas oil as a function of the operating temperature, as shown by the CO and CH_4 concentrations measured in the splash zone. However, the in-bed combustion is poorer as CH_4 and CO at the bed exit are higher.

iii. An innovative technique for the analysis of the micro–explosive regime is presented. It consists in the comparison of oxygen concentration measured by the zirconia-based probes at different heights in the bed and in the splash region, pressure signals measured in the freeboard and purposely filtered, and video-recordings of the bed surface phenomena. As a first result, it appears that the zirconia-based sensors prove to be a valid tool to detect the occurrence of a localized micro explosion.

iv. The splash zone must be regarded as a further reactor for the fuel oxidation past the bed zone and it must be taken in the due consideration in every effort leading to the understanding of the combustion mechanism or simulation of the low-temperature combustion process.

v. All in all, the results presented in this paper add further qualitative and quantitative information for the comprehension of the mechanism of low temperature, liquid fuel, FB combustion. They represent a further step towards the development and validation of a meaningful simulation model.

APPENDIX.

The non-dimensional Crossflow Ratio [18] is defined as:

$$X_b = \frac{H_{eb} K_{BE}}{U_{be}}.$$

The overall bubble-to-emulsion mass transfer coefficient, K_{BE}, and the bubble rise velocity, U_{be}, were referred to the mean equivalent endogenous bubble size, $\overline{D}_{be}$, evaluated by assuming for the endogenous bubble the same growing rate of an exogenous bubble.

The other relationships used in the calculations are:

Davidson and Schuler correlation for the initial bubble volume downstream from a nozzle [18]

$$V_{b0} = 1.138 \cdot \frac{Q_0^{1.2}}{g^{0.6}}$$

modified Cai et al. [19] correlation for the mean equivalent diameter of the endogenous bubble

$$\overline{D}_{be} = D_{be0} + 0.21 \cdot H_{eb}^{0.8} \cdot (U - U_{mf})^{0.42} \cdot \exp\left(-0.25 \cdot (U - U_{mf})^2 - 0.1 \cdot (U - U_{mf})\right)$$

Kunii and Levenspiel [18]correlations for bubble velocity calculation

$$U_{br} = 0.711\sqrt{9.81 \cdot D_{be}} \quad \text{for} \quad D_{be}/d_t < 0.125$$

$$U_{be} = 0.711\sqrt{9.81 \cdot D_{be}} \cdot 1.2 \cdot \exp\left(-1.49 \cdot \frac{D_{be}}{d_t}\right) \quad \text{for} \quad 0.125 < D_{be}/d_t < 0.6$$

$$U_{br} = 0.35\sqrt{9.81 \cdot D_{be}} \quad \text{for} \quad D_{be}/d_t > 0.6 \quad \text{(slug)}$$

Kunii and Levenspiel [18] correlations for bubble-to-emulsion mass transfer

$$K_{BC} = 4.5\left(\frac{U_{mf}}{\varepsilon_{mf}}\right) + 5.85\left(\frac{D^{0.5} g^{0.25}}{D_{be}^{1.25}}\right)$$

$$K_{CE} = 6.77\left(\frac{D \varepsilon_{mf} 0.711\sqrt{g D_{be}}}{D_{be}^{3}}\right)^{0.5}$$

$$\frac{1}{K_{BE}} = \frac{1}{K_{BC}} + \frac{1}{K_{CE}}$$

ACKNOWLEDGMENTS

This research was carried out under the MIUR-PRIN 2001-2003 financial support. The NOVAOL SpA is gratefully acknowledged for supplying bio-diesel free of the charge.

REFERENCES

[1]. Miccio F., Miccio M. and Olivieri G., 2001, "A Study on Bubbling Bed Combustion of Gas oil", Proc. of 16th Int. Conf. on FBC, Reno, ASME, 1076.

[2]. Miccio F., Miccio M., Olivieri G., Silvestre A., 2003, "On the Mechanism of Bubbling Fluidized-Bed Combustion of Gas Oil", Ind. & Eng. Chem. Res., 42:3973.

[3]. Johnsson F., Zijerveld R.C., Schouten J.C., van den Bleek C.M. and Leckner B., 2000, Int. J. Multiphase Flow, 26: 663.

[4]. Zukowsky W., 1999, "Acoustic Effects During the Combustion of Gaseous Fuels in a Bubbling Fluidized Bed", Combustion and Flame, 117, 629.

[5]. Zukowski W., 2001, "An acoustic method of studying sequential explosions during gas combustion in bubbling fluidized beds", Combustion and Flame, 125, pp. 1075-1082.

[6]. Zukowski W., 2002, "The Pressure Pulses Generated by the Combustion of Natural Gas in Bubbling Fluidized Beds", Combustion and Flame, 130, pp. 15-26.

[7]. Bulewicz E.M., Zukowski W., Kandefer S., Pilawska M., 2003, "Flame flashes when bubbles explode during the combustion of gaseous mixtures in a bubbling fluidized-bed", Combustion and Flame, 132, pp. 319-327.

[8]. Ljungstroem, Evert B., 1985, "In-bed oxygen measurements in a commercial-size AFBC". Proceedings of the International Conference on Fluidized Bed Combustion 8th (2), 853-64.

[9]. Sterneus, J.; Johnsson, F.; Leckner, B.; Wiesendorf, V.; Werther, J., 2000, "Measurements of fluid dynamics and reaction conditions in the bottom zone of large-scale CFB combustors", Journal of the Institute of Energy, 73 (497), 184-190.
[10]. Stubington, J. F.; Chan, S. W., 1990, "The interpretation of oxygen-probe measurements in fluidized-bed combustors". Journal of the Institute of Energy, 63(456), 136-42.
[11]. Stubington, John F., Clough, Stephen J., 1997, "The combustion rate of volatiles in a fluidized bed combustor. Proceedings of the International Conference on Fluidized Bed Combustion", 14th (Vol. 2), 1111-1122.
[12]. Solimene R., Passarelli G., Marzocchella A., Salatino P., 2004, "Diagnostics of gas-mixing in a bubbling gas-fluidized bed by means of zirconia-based oxygen sensors", submitted for publication to AIChE J.
[13]. Malato M., M. Miccio and F. Miccio, 2003, "Passive Measurements of Time-variable Signals of Pressure During FB Combustion of Liquid Fuels", Proc. of the Joint Meeting of the Scandinavian-Nordic and Italian Sections of the Combustion Institute, pp. 4.7.1-4, ISBN 88-88104-04-6, Ischia (I), Sept. 18-21.
[14]. Moseley P.T., Norris, J., Williams D.E., 1991, "Techniques and mechanisms in gas sensing", Adam Hilger.
[15]. Fiorentino M., Mazzocchella A., Salatino P., 1997, "Segregation of fuel particles and volatile matter during devolatilization in a fluidized bed reactor", Chem. Eng. Science, 52, 1893.
[16]. Frassoldati A., Faravelli T., Miccio F., Miccio M. and Ranzi E., "Modeling homogeneous combustion in bubbling beds burning liquid fuels", Paper FBC2003-133, Proc. of 17th Int. Conference on FBC, Jacksonville, Florida (USA), published on CD-ROM by ASME, ISBN 0-7918-3675-4, May 18-21, 2003
[17]. Merry J.M.D., "Penetration of a Horizontal Gas Jet into a Fluidised Bed" Trans. Inst. Chem. Eng., 49, pp. 189-195, 1971.
[18]. Kunii D., Levenspiel O., 1991, "Fluidization Engineering 2. ed.", Butterworth-Heinemann.
[19]. Cai P., Schiavetti M., De Michele G., Grazzini G.C., Miccio M., 1994, "Quantitative Estimation of Bubble Size in PFBC", Powd. Tech., 80, pp. 99-109.